TRENDS IN SCIENCES 2025; 22(6): 9782 RESEARCH ARTICLE
https://doi.org/10.48048/tis.2025.9782

Synthesis and Characterization of Nanochitosan-Based Smart Film as Future Food Packaging Material

Hasri[1,*], Pince Salempa[1], Nurhayani[2], Suriati Eka Putri[1], Eka Risdayanti[3], Satria Putra Jaya Negara[1] and Elvira Masarrang[3]

[1]Department of Chemistry, Faculty of Mathematics and Natural Science, Universitas Negeri Makassar, South Sulawesi, Indonesia
[2]Science Education Study Program, Faculty of Mathematics and Natural Science, Universitas Negeri Makassar, South Sulawesi, Indonesia
[3]Students of Chemistry Department, Faculty of Mathematics and Natural Science, Universitas Negeri Makassar, South Sulawesi, Indonesia

([*]Corresponding author's e-mail: hasriu@unm.ac.id)

Received: 16 January 2025, Revised: 5 February 2025, Accepted: 12 February 2025, Published: 10 May 2025

Abstract

Recent developments of materials for food packaging have been attempted to utilize biodegradable materials such as nanochitosan. The composite film of nanochitosan can be synthesized with various suitable materials. In this particular study, nanochitosan was paired with polyethylene glycol (PEG) because PEG has the ability to strengthen nanochitosan film. This study aims to determine the characteristics of nanochitosan and nanochitosan-PEG in an effort to develop smart edible film designed to monitor food freshness. Several stages had been conducted, it all began with the synthesis of nanochitosan and nanochitosan-PEG. The samples of nanochitosan-PEG were conditioned consecutively with various PEG concentrations of 1, 1.5 and 2 %. Nanochitosan and nanochitosan-PEG were characterized by using Fourier Transform Infrared (FTIR), Particle Size Analyzer (PSA), and Structural Equation Modeling (SEM) spectrophotometer, while stability was tested with a UV-Vis spectrophotometer. The results of FTIR interpretation showed the functional groups like -OH, -NH, C=O carboxylate, P=O, and C-O-C. These functional groups featured a fairly sharp absorption peak implying the characteristic of PEG. The PSA test revealed that the nanochitosan-PEG 2 % obtained the smallest particle size. The treatment of time variations was required to react the nanochitosan-PEG 2 % with the ionic gelation method within 30, 60, and 120 min. After a 2-hour reaction, the smallest size particle reached 9.78 nm with a polydispersity index value of 0.021. The morphology of samples in the SEM test showed non-uniform spherical aggregates. The film yield proceeded to use on chicken meat for indicating the meat's freshness. It took 48 h signifying a decline of protein content from 18.30 to 15.86 % as the film experienced a color change from purple to green according to the pH level of the decaying meat. This suggests that the film is smart and reliable to monitor food freshness through visual pH changes.

Keywords: Smart Film, Future food packaging, Ionic gelatin, Nanochitosan, Nanochitosan-PEG

Introduction

The food packaging industry has been responsible to the massive and uncontrolled use of petroleum-based materials such as plastics. Plastics continously perpetuate a serius enviromental problem. Researchers have been encouraged to develop new biomaterials that explore the emerging concept of sustainable development. Chitosan is a biopolymer derived from chitin, which is widely distributed in nature and is the second most abundant polysaccharide after cellulose [1]. Chitosan offers immense advantages as an edible

packaging material owing to its good film-forming properties and low toxicity; it can also be an excellent vehicle for incorporating a wide variety of additives [2].

The manufacture of nanochitosan requires the addition of triphosphate (TPP) which functions as a crosslinking agent to strengthen the matrix [3,4]. To enhance the stability of the material, polymers such as polyethylene glycol (PEG) are often incorporated [5,6]. PEG can bind water, with the extent of blinding dependent on its molecular weight and concentration [7,8].

Several methods have been developed for producing nanochitosan such as microemulsion and sonication. The microemulsion is time-consuming and requires complex nanochitosan washing stages [9,10], Sonication, despite being widely used demands significant energy and costs, while the particle size produced tends to be larger than the ionic gelation method [11,12]. Additional methods, such as solvent diffusion emulsification using magnetic stirring and high-pressure homogenization, have also been explored [13,14]. This study uses ionic gelation to minimize the limitations of other methods. Ionic gelation is a simple and efficient synthesis process that includes chemical reactions in solution without heating at high temperatures. It is easily controlled without using dangerous organic solvents, requires low energy, and is relatively inexpensive [11,15].

Synthesis of nanochitosan with the addition of PEG improves the stability. This is because the compound contains an O atom in the hydroxyl chain structure, which interacts with cations in chitosan. The interaction produces particles measuring 1 - 100 nanometers, with morphological size of less than 1,000 nm in the form of balls [6,16,17]. Extended stirring further reduces the size by breaking down larger particles into nanoscale dimensions, with nanochitosan measuring 85.3 nm and a polydispersity index value of 0.287 [18-20].

Chitosan modification into nano form is utilized as a filler in edible formulations to enhance antibacterial activity. Nanochitosan can also be combined with other materials to obtain edible films with superior mechanical and functional properties [21,22]. At low concentrations, nanochitosan disperses effectively in edible solutions, contributing to better film formation [12].

To meet consumer needs for fresh, clean, safe, and quality food ingredients, the development of smart packaging with integrated colorimetric indicators has gained significant attention [23,24]. In this study, an edible film was developed in the form of smart food packaging, utilizing anthocyanin extract as a colorimetric indicator to monitor the freshness of chicken meat during storage.

Materials and methods

Materials

The materials used in this study were Merck chitosan, concentrated glacial acetic acid (CH_3COOH), anthocyanin extract, Merck glycerol ($C_3H_8O_3$), Sigma-Aldrich sodium tripolyphosphate (Na-TPP), Merck tween 80 and Merck PEG 6,000.

Methods

Synthesis of nanochitosan and nanochitosan-PEG with concentration variations (1, 1.5 and 2 %)

First and foremost, the preparation of of nanochitosan sample was conducted by dissolving 0.1 g of chitosan in 100 mL of 1 % (v/v) acetic acid and it required stirring for 1 h. Then the solution was mixed with 10 mL of 0.15 % NaTPP (w/v) and 0.5 mL of tween 80. This step required stirring for 2 h. The 1st mixture would become the nanochitosan sample. Secondly, the preparation of 3 nanochitosan-PEG samples were obtained by repeating the exact procedures like the 1st sample. However, various concentrations of 1 mL PEG solution were added in the end to each mixture. There were 1, 1.5 and 2 % (w/v) PEG solution consecutively for each of nanochitosan-PEG samples. These samples required stirring for 30 min [25,26]. The following images presented in **Figure 1** are to better comprehend the procedures of synthesizing nanochitosan-PEG.

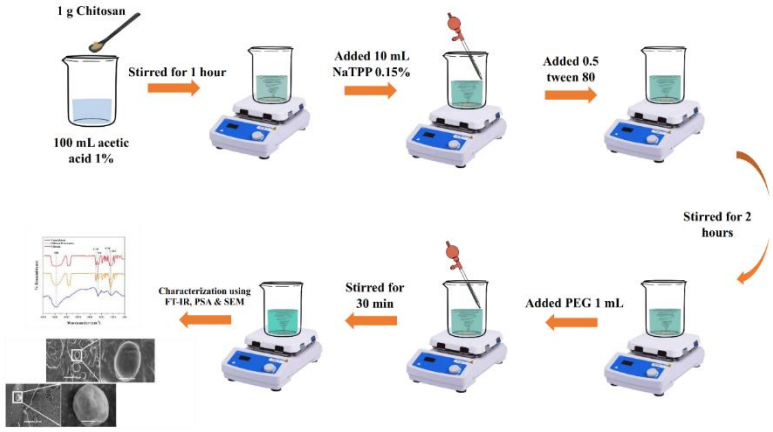

Figure 1 The synthesis procedures of nanochitosan-PEG.

Characterization of nanochitosan and nanochitosan-PEG using FTIR and PSA spectrophotometer

Fourier Transform Infrared (FTIR) spectrophotometer (Prestige-21, Shimadzu) characterization was conducted to determine the degree of chitosan deacetylation. It was calculated by combining the baseline determination method on the A_{1655}/A_{3450} absorption band [27] as shown by the following equation.

$$\%\ DD = 100 - \left(\frac{A1655}{A3450} \times \frac{1}{1.33}\right) \quad (1)$$

FTIR characterization provided information of the functional groups that belong to chitosan, nanochitosan, and nanochitosan-PEG. The vibration and rotation of molecules influenced by infrared radiation at a particular wavelength could identify structural differences in molecular binding between entities, which can reveal details about the existence of their interactions.

Particle Size Analyzer (PSA) (Horiba SZ-100) was also conducted for the characterization. It was able to determine particle sizes and polydispersity index values of nanochitosan and nanochitosan-PEG with various concentrations consecutively of 1, 1.5 and 2 %. When the result obtains the smallest polydispersity index value, it would be further tested with various reaction times.

Morphological analysis of the smart film using SEM (JSM-6510LA-EX-3618OD3A) was required to observe the surface and microstructure of the film. This allowed researchers to evaluate homogeneity, porosity, and the presence of cracks or imperfections at micrometer scales.

Application of nanochitosan-PEG in indicating food freshness

The method for this application started off by dissolving chitosan with 1 % acetic acid [28]. The solution was stirred using a magnetic stirrer at a speed of 750 rpm and a temperature of 80 °C for 45 min. Furthermore, 0.2 g of PEG and 1 mL of anthocyanin extract were added. The mixture was added with glycerol at a concentration of 3 % [29]. The film solution was poured into a Teflon plate to mold and then it required an oven to dry at a temperature of 50 °C for 24 h. Later the film obtained was attached to the top part of a petri dish where the chicken meat was put or packaged. The film attempted to act smartly as an indicator of meat freshness. The sample used was chicken breast meat aged 1.5 - 2 months.

Indicating the freshness of meat in this study is asscoicated with a change in pH implying the meat has started to decay. So, the smart film as the indicator required a pH standar. In order to make the standardization of pH on the smart film, certain addition of solutions needed to mix beforehand such as 11.88 mL of nanochitosan, 1.25 mL of anthocyanin extract, 1 mL of PEG 2 %, and 3 mL of pH solution ranging from 2 to 11. This process attained 10 different standardized films consecutively based on each addition of pH solutions.

Kjeldahl test

Kjeldahl testing was carried out at the Makassar Health Laboratory using SNI ISO 1871:2015.

Results and discussion

Nanochitosan and nanochitosan-PEG were synthesized by the ionic gelation method. This aimed to obtain chitosan powder with a uniform size as shown in **Figure 2**.

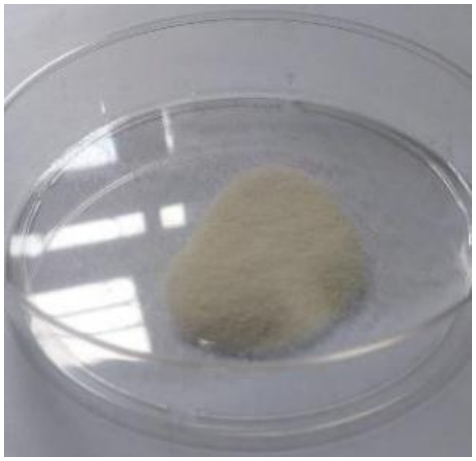

Figure 2 The result of sieved chitosan at a mesh of ≤ 100.

Prior to the synthesis of nanochitosan and nanochitosan-PEG, the degree of deacetylation (DD) of chitosan was determined to learn the percentage acetyl groups lost in the deacetylation process. In other words, the DD value suggested the purity of chitosan. This was based on the results of the FTIR test in **Figure 3** which plot the baseline on the absorption band A_{1655}/A_{3450}. A_{1655} is the absorbance value at a wavenumber of 1,650 - 1,500 cm^{-1} corresponding to NHCO group while A_{3450} is the absorbance value at a wavenumber of 3,500 - 200 cm^{-1} [30]. Therefore the degree of deacetylation of chitosan reached a percentage of 88.6 %. The higher the DD value, the more amino groups existed in the chitosan molecule. This could make the chitosan more reactive.

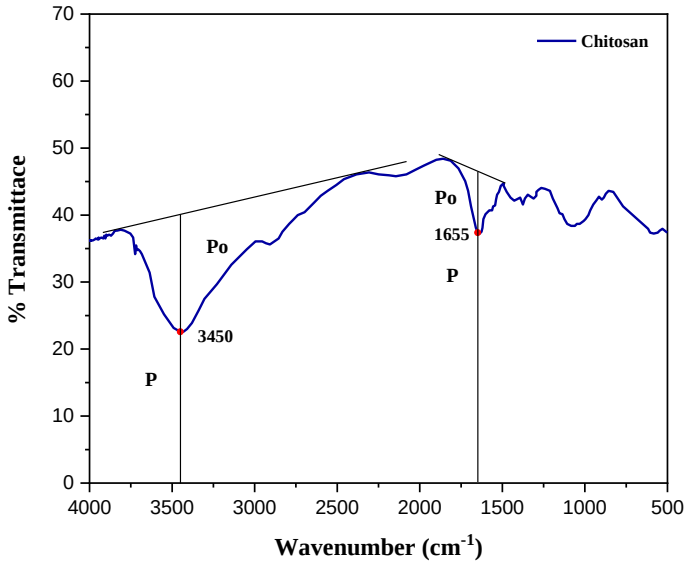

Figure 3 FTIR spectroscopy of chitosan.

The mechanism of nanochitosan formation relies on the interaction between the positively charged chitosan and the negatively charged tripolyphosphate as shown in **Figure 4**. In acidic conditions, chitosan

becomes protonated which is able to produce NH_3^+ ions. Then it interacts electrostatically with the oxygen atom of NaTPP. Crosslinking occurs through these ionic interactions between the cationic chitosan and the anionic tripolyphosphate ions. Treating nanochitosan under acidic conditions is essential in order to create these strong electrical interactions [31].

The addition of PEG functions as a stabilizer [6]. The compound contains oxygen atoms (O) in the chain structure and hydroxyl groups (-OH) that interact with cations in chitosan [32-35].

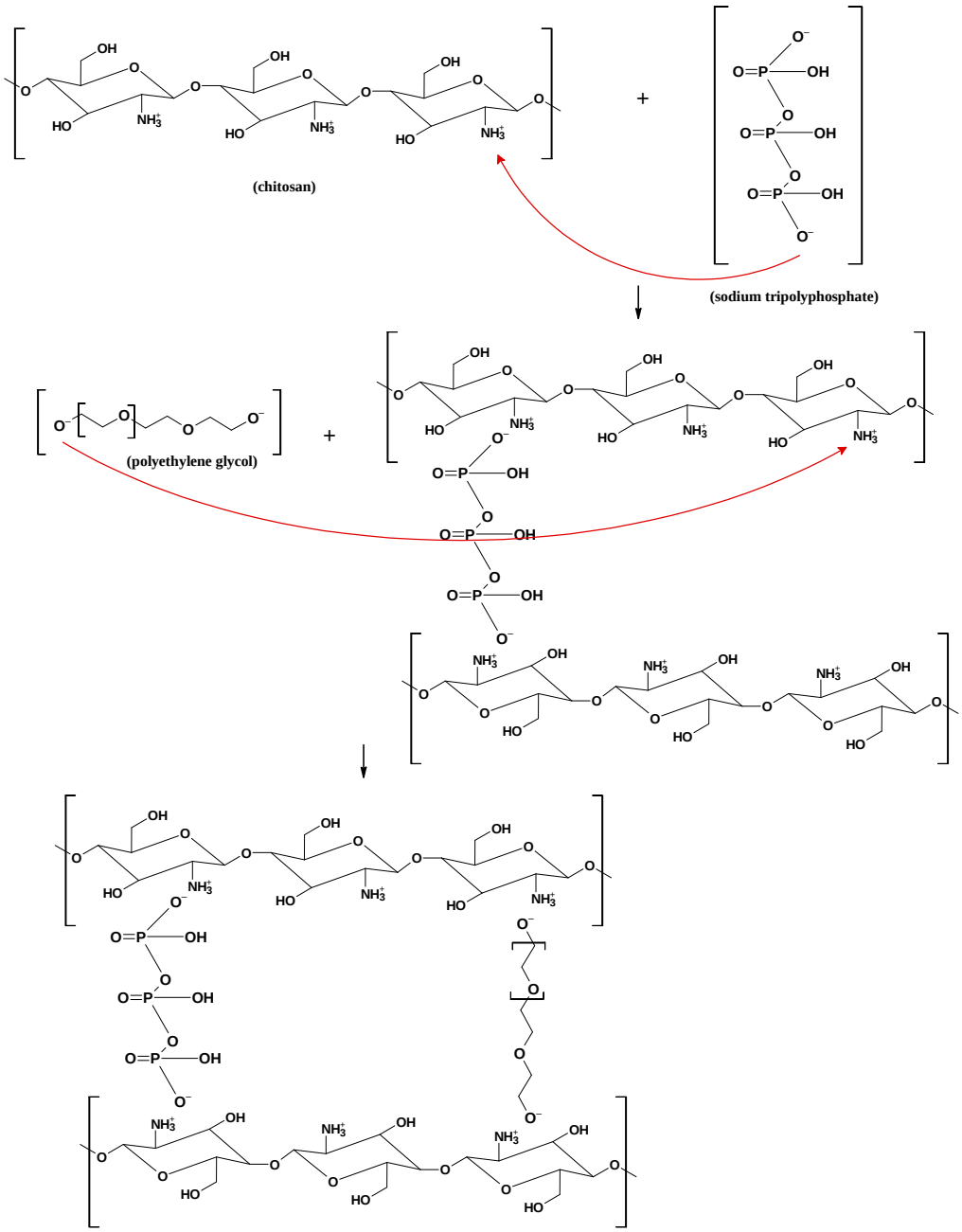

Figure 4 The mechanism of nanochitosan and nanochitosan-PEG interaction.

FTIR analysis of nanochitosan and nanochitosan-PEG

FTIR spectroscopy was adopted to identify the functional groups present in the nanochitosan-PEG compound. This analysis was conducted across a wavenumber range of 4,000 - 500 cm^{-1}. FTIR spectroscopy of chitosan, protonated chitosan and nanochitosan is shown in **Figure 5**.

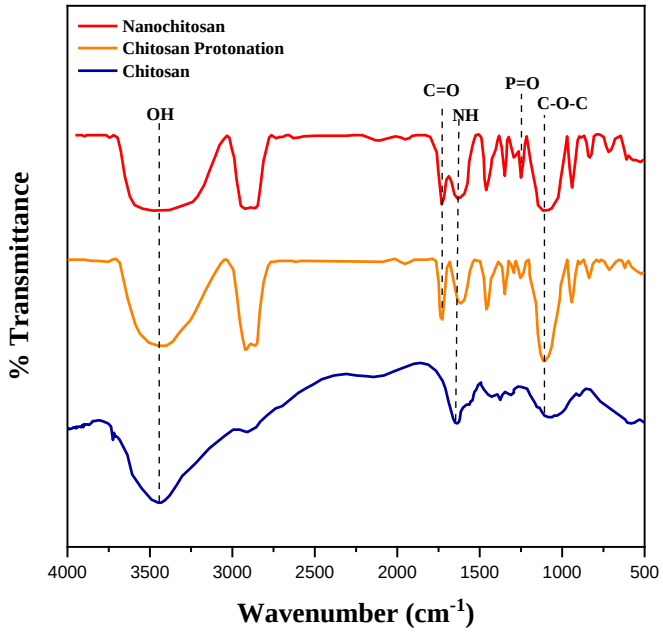

Figure 5 FTIR spectroscopy of chitosan, protonation of chitosan and nanochitosan.

Table 1 FTIR spectroscopy data of chitosan, protonation of chitosan and nanochitosan.

Types of absorption	Reference	Wavenumber (cm^{-1})		
		Chitosan	Protonation of chitosan	Nanochitosan
OH	3,200 - 3,600*	3,449.63	3,441.01	3,439.08
NH amine bend	1,575 - 1,650**	1,638.36	1,649.35	1,639.49
Carboxylate C=O Stretch	1,700 - 1,725**	-	1,734.93	1,735.93
P=O Extension	1,200 - 1,500**	-	-	1,249.87
C-O-C	1,320 - 1,000***			

*[26], **[36], ***[37].

The spectrum of chitosan shows an absorption at 1,638.36 cm^{-1}, corresponding to the bending vibration of N-H at wavenumber 3,449.63 cm^{-1}. N-H and -OH groups are characteristic of chitosan because based on the molecular structure it has both hydroxyl group -OH and HN groups [38,39]. After chitosan is bound to acetic acid, a new absorption appears at 1,735.95 cm^{-1}, representing the stretching vibration of the carbonyl group C=O carboxylate. This peak signified the interaction of acetic acid with chitosan through O- atom and NH_3^+, respectively [40]. The presence of chitosan crosslinked with NaTPP is proven by the emergence of new absorption in the P=O stretching vibration with a wavenumber of 1,249.87 cm^{-1}. This indicates that the NH_2 group protonated into NH_3^+ chitosan has been crosslinked with the oxygen atom of NaTPP [41].

Subsequent testing with FTIR includes a few nanochitosan samples modified with PEG at various concentrations consecutively of 1, 1.5 and 2 %. It also includes the nanochitosan-PEG 2 % subjected to various reaction times of 30, 60, and 120 min. Based on the FTIR spectroscopy, the spectrums of nanochitosan with the treatment of concentration variations are presented in **Figure 6**. Meanwhile in **Figure 7** exhibits the spectrums of primarily nanochitosan 2 % with the treatment of time variations. The data in **Table 2** provides types of absorption and their wavenumbers which is divided into 2 groups, the concentration variations and the time variations.

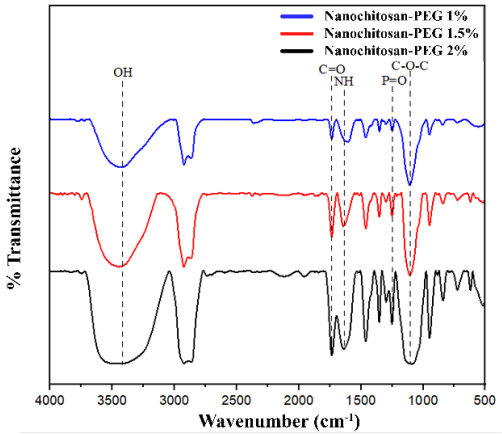

Figure 6 FTIR spectroscopy of nanochitosan-PEG with concentration variations (1, 1.5 and 2 %).

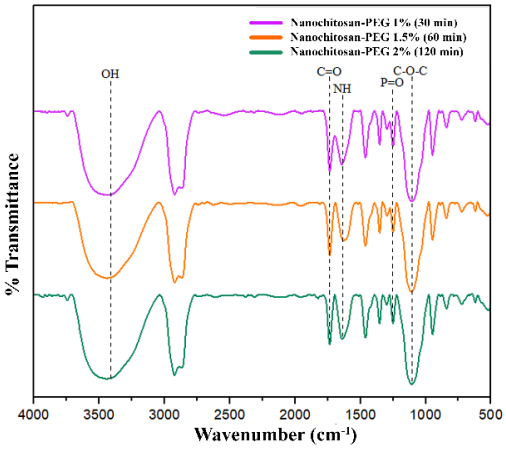

Figure 7 FTIR spectroscopy of primarily nanochitosan-PEG 2 % with time variations (30 min, 60 min, and 120 min).

Table 2 FTIR spectroscopy data of nanochitosan samples with concentration variations and nanochitosan-PEG 2 % samples with time variations.

Types of absorption	Reference	Wavenumber (cm^{-1})					
		Nanochitosan samples with concentration variations			Nanochitosan-PEG 2 % samples with time variations		
		1 %	1.5 %	2 %	30 min	60 min	120 min
OH	3,200 - 3,500*	3,435.22	3,446.79	3,444.87	3,442.94	3,441.01	3,442.94
Bend NH Amin	1,640 - 1,560**	1,620.21	1,634.35	1,639.49	1,643.35	1,625.99	1,639.49
C=O Carboxylate	1,730 - 1,700**	1,735.93	1,735.93	1,734.01	1,734.01	1,735.93	1,735.93
P=O Extension	1,200 - 1,500**	1,249.87	1,249.87	1,249.87	1,249.87	1,249.87	1,249.87
C-O-C ether stretch	1,320 - 1,000***	1,109.07	1,107.14	1,093.64	1,105.21	1,109.07	1,105.21

*[26], **[36], ***[42].

The results of FTIR spectroscopy on each nanochitosan-PEG sample with comcemtratom variations and stirring time showed a shift in wavelength. This suggested the presence of a fairly sharp C-O-C ether functional group which was a characteristic of PEG [43]. C-O-C spectrum was in the range of 1,320 - 1,000 cm^{-1} [44]. It was important to acknowledge that there was no significant difference in functional groups in all variations of nanochitosan-PEG samples. Previous studies identified a fairly sharp C-O-

C ether functional group in the 1,095.57 cm^{-1} region [43,44], confirming that PEG was bound to chitosan. The interaction was further characterized by the NH and OH spectrum [45].

The presence of OH, NH, C=O carboxylate, P=O, and C-O-C functional groups shows that nanochitosan has formed and structurally bonded with PEG. The absorption of OH groups appeared at 3,367.1 cm^{-1} which was a characteristic of chitosan [26]. Meanwhile, the P=O group appeared at wave number 1,145.51 cm^{-1} with the presence of a fairly sharp ether group C-O-C, which was a characteristic of PEG [43,44].

PSA analysis of nanochitosan and nanochitosan-PEG

Analysis of nanochitosan-PEG using PSA was conducted to determine particle size. The results of PSA tests of nanochitosan and nanochitosan-PEG with various PEG concentrations of 1, 1.5 and 2 %, are shown in **Table 3**.

Table 3 PSA test results of nanochitosan and nanochitosan-PEG with concentration variations.

No	Synthesis of nanochitosan-PEG	Polydispersity index	Average particle size (nm)
1	Nanochitosan	0.6021	10.44
2	Nanochitosan-PEG 1 %	0.5450	10.22
3	Nanochitosan-PEG 1.5 %	0.6101	10.12
4	Nanochitosan-PEG 2 %	0.1211	9.70

Synthesis of nanochitosan, generated particles with an average size of 10.44 nm and a polydispersity index of 0.6021. Variations in the concentration of nanochitosan-PEG, using the ionic gelation method, produced particle sizes ranging from 9.70 - 10.22 nm. These measurements confirmed that both nanochitosan and nanochitosan-PEG fell in the nanomaterial range of 1 - 100 nm [46,47]. The downward trend in particle size as the PEG concentration increases is due to the PEG's capacity to bind water through -OH groups and long-chain structure, which enhances the homogeneity of nanochitosan [48]. PEG coats the chitosan surface and greatly affects the van der Waals forces and increases the repulsive forces. This causes gradual reduction in particle size and prevents aggregation.

The results of the first PSA test dictates the 2nd one. The smallest particle size was obtained by nanochitosan-PEG 2 %. Further treatment for this particular concentration is required to react within selected time variations. The results of PSA test with various reaction times are shown in **Table 4**.

Table 4 PSA test results of nanochitosan-PEG 2 % with time variations.

No	Synthesis of nanochitosan-PEG 2 %	Polydispersity index	Average particle size (nm)
1	30 min	0.0443	9.93
2	60 min	0.0410	9.84
3	120 min	0.0214	9.78

Synthesis of nanochitosan-PEG 2 % with time variations using the ionic gelation method obtained particles ranging in size from 9.78 to 9.93 nm. This confirmed that nanochitosan-PEG falls in the nanomaterial range of 1 - 100 nm [46,47]. Additionally, the stirring time increases as particle size decreases. The trend is attributed to the progressive breakdown of larger particles into smaller, nano-sized particles [49].

Characterization using structural equation modeling (SEM)

Nanochitosan and nanochitosan-PEG variations in concentration and time were analyzed morphologically by using SEM. The results are shown in **Figure 8(a)** Morphology of nanochitosan at 100× and 500× magnification (b) Morphology of nanochitosan-PEG 2 % at 100× and 3,000× magnification and (c)

Morphology of nanochitosan-PEG 2 % after a 2-hour reaction at 100× and 500× magnification.

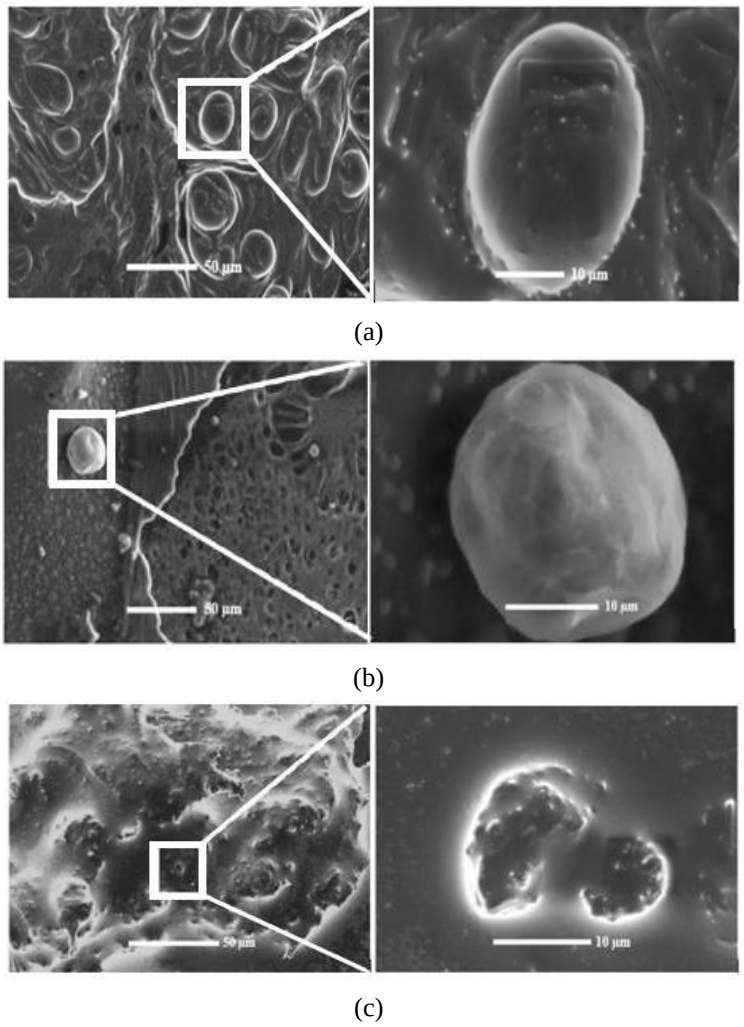

Figure 8 (a) Morphology of nanochitosan at 100× and 500× magnification. (b) Morphology of nanochitosan-PEG 2 % at 100× and 3,000× magnification, and (c) Morphology of nanochitosan-PEG2 % after a 2-hour reaction at 100× and 500× magnification.

The results of SEM analysis showed a morphology in the form of small, non-uniform (heterogeneous) circles forming nanochitosan aggregates [50]. The ionic gelation method includes dissolving chitosan in a dilute acid and then adding TPP solution with a different charge, specifically polycationic. This led to the complexation of different charges, causing ionic gelation and precipitation to form round particles such as balls [51]. The non-uniform shape is caused by the coagulation effect of nanochitosan [9].

Stability test of nanochitosan, nanochitosan-PEG 2 %, and nanochitosan-PEG 2 % 120 min with UV-Vis

UV-Vis spectrophotometer was used to determine the stability of nanochitosan, nanochitosan-PEG 2 %, and nanochitosan-PEG 2 % after a 120-minute reaction where each one had been observed within 5 periods (1, 2, 3, 4 and 5 days). This test obtained wavenumbers as displayed in the following bar graph in **Figure 9**.

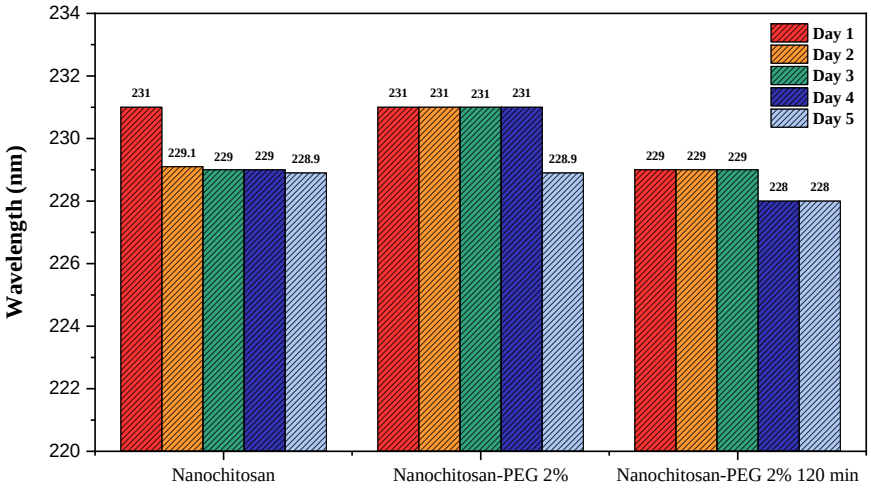

Figure 9 Stability graph of nanochitosan, nanochitosan-PEG 2 %, and nanochitosan-PEG 2 % 120 min using UV-Vis.

For nanochitosan, the wavelength started off with 231 nm and decreased at a wavelength of 229.1 in day 2 and remained relatively constant afterward with a minor decrease at wavelength of 228.9 nm in day 5. For nanochitosan-PEG 2 %, the wavelength stayed at a number of 231 nm throughout 4 days period, and then changed at a wavelength of 228.9 nm in day 5. Meanwhile, the wavelength for nanochitosan-PEG 2 % 120 min initially remained at a wavelength of 229 nm only for 3 days period but decreased in day 4 to a wavelength of 228 nm. The decrease of wavenumbers that belongs to nanochitosan, nanochitosan-PEG 2 %, and nanochitosan-PEG 2 % 120 min is not significant. This suggests the stability of the 3 entities.

The best stability goes to nanochitosan-PEG 2 %, which is characterized by no decrease in wavenumber for 4 days. This shows how the protective capacity of PEG-6000 works during the storage period [14,57]. This reinforces the fact that PEG have the capacity to stabilize or to aggregrate particles in order to coat chitosan surface. The wavelength is directly proportional to the size of nanochitosan [52,53]. This reflects a reduction in size and prevents the aggregation process of particles [54]. A shorter wavelength will cause a higher number of scatterings, and a smaller particle size will produce lower energy resonances.

Application of nanochitosan-PEG 2 % after a 2-hour reaction in indicating food freshness

The yield of nanochitosan-PEG after 2-hour reaction was chosen to apply as an indicator of food freshness. The smart film appeared to be transparent in the shape of 2×5 cm rectangular with a thickness of 0.08 mm as shown in **Figure 10**.

Figure 10 The physical appearance of nanochitosan-PEG as a smart film.

Freshness of food especially in this study is indicated through visual pH changes of the film. It is essential to standardize pH solely for the film first before the application begins. Several solutions such as

nanochitosan, anthocyanin extract, PEG 2 % are mixed to attain the following standardized films in **Figure 11** consecutively based on each addition of pH solutions ranging from 2 to 11.

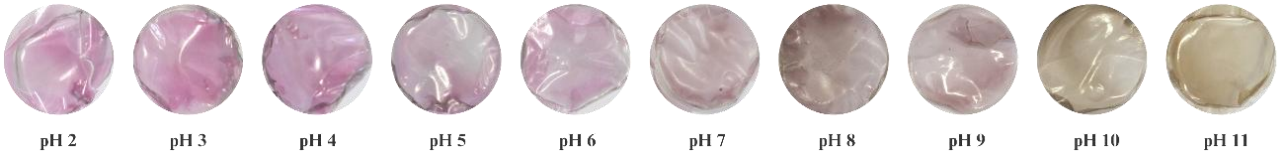

Figure 11 Fabrication of the smart films as the pH standard.

The results of standardized process for the smart films signify a variety of colors as shown in **Figure 11**. The pH 2 standard appears purple and changes color most visibly after the pH 8 standard. Later this standardization of the smart films can be referenced when indicating food freshness.

The application of the smart film in indicating food freshness specifically used chicken meat. Visual and olfactory changes were observed within 0, 24 and 48 h at a room temperature as shown in **Figure 12**.

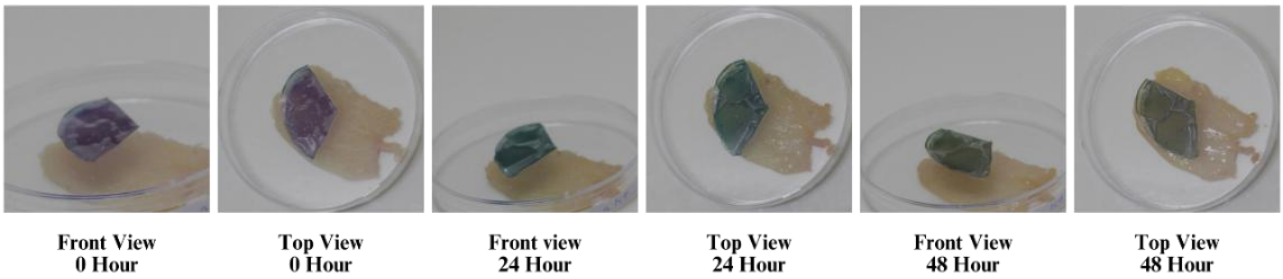

Figure 12 The application of smart film for chicken meat at 0, 24, and 48 h.

The smart film initially matches pH 6 and changes over time to pH 10. According to the colors of pH standard, the smart film appears purple when it's still fresh (0 h), changes to dark green as the meat begins to develop a fishy odor (24 h), and eventually turns brownish green as the chicken rots away and its texture deteriorates. The increase in pH is caused by microbial activity, which breaks down amino acids and produces basic compounds such as ammonia or NH_4 [23,55,56].

The last requirement for this study is the Kjehdal test. It is a method to determine nitrogen levels in a sample, especially to measure protein content in food, animal feed, or other organic materials. The protein content of fresh chicken meat and chicken meat after 2 days of storage are presented in **Table 5**.

Table 5 Protein content of chicken meat.

No	Sample	Protein content (%)
1	Day 0 chicken meat	18.30
2	Day 2 chicken meat	15.86

Storage condition affects the protein content of chicken meat through various chemical, physical and microbiological mechanisms. During storage, especially at room temperature or uncontrolled temperatures, proteolytic enzymes and microorganism activity can break down proteins into peptides and free amino acids, reducing total protein content. Long-term storage can also trigger the Maillard reaction and protein oxidation, especially when meat is not properly packaged.

Conclusions

The synthesis of nanochitosan and nanochitosan-PEG has been successfully carried out by mixing chitosan, NaTPP, tween 80, PEG and anthocyanin extract. The concentrations of PEG varied at 1, 1.5 and 2 % consecutively to obtain nanochitosan-PEG. The characterization with FTIR indicates the presence of functional groups like OH, NH, C=O carboxylate, P=O, and C-O-C which confirms that nanochitosan has formed and structurally bonded with PEG. The characterization with PSA shows that the result of downward trend in particle size as the PEG concentration increases reinforces the idea that PEG can bind water through -OH groups and long-chain structure. PEG has protective capacity where it coats nanochitosan surface, makes gradual reduction in particle size, and prevents aggregation. Subsequent characterization of PSA was conducted to react nanochitosan-PEG 2 % within 30, 60 and 120 min. The optimum time of nanochitosan PEG reached after 120 min as the result shows the smallest particle size of 9.78 nm. Morphological results with SEM show non-uniform particles that are spherical or round-shaped. The stability test with UV-Vis reveals that nanochitosan-PEG 2 % can endure the same wavenumber for 4 days. The smart film application of nanchitosan-PEG in indicating food freshness concludes that the film wields the smart capacity to indicate pH of chicken meat. Based on the pH standard, the smart film matches the purple color signifying pH 6 and over 48 h changes to brownish green signifying pH 10. The meat experiences a decline in quality over time as pH of the meat changes due to the microbial growth.

Acknowledgements

The authors are grateful to DRTPM Ministry of Education, Culture, Research, and Technology Republic of Indonesia in the scheme of Fundamental Research Scheme contract number 2859/UN36.11/LP2M/2024 and Lembaga Penelitian and Pengabdian Masyarakat (LP2M) Universitas Negeri Makassar, Indonesia, that has held writing workshops of scientific articles in reputable international journals, for supporting this study.

References

[1] M Flórez, E Guerra-Rodríguez, P Cazón and M Vázquez. Chitosan for food packaging: Recent advances in active and intelligent films. *Food Hydrocolloids* 2022; **124**, 107328.

[2] DCM Ferreira, ALD Souza, JVWD Silveira, FM Pelissari, BM Marim, GAG Giraldo, J Mantovan and S Mali. *Multifunctional hybrid nanomaterials for sustainable agri-food and ecosystems: A note from the editor. In*: KA Abd-Elsalam (Ed.). Multifunctional hybrid nanomaterials for sustainable agri-food and ecosystems: A volume in micro and nano technologies. Elsevier, Amsterdam, Netherlands, 2020, p. 393-435.

[3] M Alfatama, H Choukaife, H Alkhatib, O Al Rahal and NZM Zin. A comprehensive review of oral chitosan drug delivery systems: Applications for oral insulin delivery. *Nanotechnol* 2024; **13(1)**, 20230205.

[4] P Sitarek, T Kowalczyk, M Owczarek and L Herczy. Combination with ginkgo biloba extract in preliminary *in vitro* studies. *Molecules* 2023; **28(13)**, 4950.

[5] Z Jamalpoor, H Ahmadi, M Heydari, M Abdouss, A Rahdar and AM Díez-Pascual. Chitosan based niosomal hydrogel with polyethylene glycol and halloysite nanotubes for curcumin delivery. *Journal of Molecular Liquids* 2024; **401(9)**, 124640.

[6] MK Amin and JS Boateng. Enhancing stability and mucoadhesive properties of chitosan nanoparticles by surface modification with sodium alginate and polyethylene glycol for potential oral mucosa vaccine delivery. *Marine Drugs* 2022; **20(3)**, 156.

[7] SV Khairnar, P Pagare, A Thakre, AR Nambiar, V Junnuthula, MC Abraham, P Kolimi, D Nyavanand and S Dyawanapelly. Review on the scale-up methods for the preparation of solid lipid nanoparticles. *Pharmaceutics* 2022; **14(9)**, 1886.

[8] SA Gaballa, Y Naguib, F Mady and K Khaled. Polyethylene glycol: Properties, applications, and challenges. *Journal of Advanced Biomedical and Pharmaceutical Sciences* 2023; **7**, 26-36.

[9] DV Abere, SA Ojo, MB Paredes-Epinosa and A Hakami. Derivation of composites of chitosan-nanoparticles from crustaceans source for

nanomedicine: A mini review. *Biomedical Engineering Advances* 2022; **4(3)**, 100058.

[10] NAI Muddin, MM Badsha, MA Arafath, ZMA Merican and MS Hossain. Magnetic chitosan nanoparticles as a potential bio-sorbent for the removal of Cr(VI) from wastewater: Synthesis, environmental impact and challenges. *Desalination and Water Treatment Journal* 2024; **319**, 100449.

[11] NH Hoang, TL Thanh, R Sangpueak, J Treekoon, C Saengchan, W Thepbandit, NK Papathoti, A Kamkaew and N Buensanteai. Chitosan nanoparticles-based ionic gelation method: A promising candidate FOR plant disease management. *Polymers* 2022; **14(4)**, 662.

[12] SM Bashir, GA Rather, A Patrício, Z Haq, AA Sheikh, MZ ul H Shah, H Singh, AA Khan, S Imtiyaz, SB Ahmad, S Nabi, R Rakhshan, S Hassan and P Fonte. Chitosan nanoparticles: A versatile platform for biomedical applications. *Materials* 2022; **15(19)**, 6521.

[13] SH Reddy, MS Umashankar and N Damodharan. Formulation, characterization and applications on solid lipid nanoparticles - a review. *Research Journal of Pharmacy and Technology* 2018; **11(12)**, 5691-5700.

[14] A Pasban, M Mohebbi, SF Mousavi, A Rezaei, M Khalilian-Movahhed and R Mozafarpour. Effect of high-pressure homogenization treatment and Persian gum on rheological, functional properties and release kinetic of crocin from double emulsions. *LWT-Food Science and Technology* 2023; **187**, 115370-115381.

[15] SWH Shah, S Imran, I Bibi, K Ali and N Bashir. Investigations of the eutectic formation and skin rejuvenation by hyaluronan e kojic acid dipalmitate system. *Karbala International Journal of Modern Science* 2024; **10(1)**, 118-130.

[16] J Frigaard, JL Jensen, HK Galtung and M Hiorth. The potential of chitosan in nanomedicine: An overview of the cytotoxicity of chitosan based nanoparticles. *Frontiers in Pharmacology* 2022; **13**, 880377.

[17] SE Putri, A Ahmad, I Raya, RT Tjahjanto and R Irfandi. Synthesis and antibacterial activity of chitosan nanoparticles from black tiger shrimp shells (*Penaeus monodon*). *Egyptian Journal of Chemistry* 2023; **66(8)**, 129-139.

[18] H Marta, DI Rizki, E Mardawati, M Djali, M Mohammad and Y Cahyana. Starch nanoparticles: Preparation, properties and applications. *Polymers* 2023; **15(5)**, 19-25.

[19] W Taurina, R Sari, UC Hafinur, S Wahdaningsih and I Isnindar. Optimization of stirring speed and stirring time toward nanoparticle size of chitosan-siam citrus peel (*Citrus nobilis* L.var Microcarpa) 70 % ethanol extract. *Traditional Medicine Journal* 2017; **22(1)**, 16.

[20] H Ummas, DE Pratiwi, SE Putri and Alimin. Adsorption study for removal of acid orange dye using modified nano chitosan. *Journal of Physics: Conference Series* 2019; **1244(1)**, 012034.

[21] VSD Santos, MV Lorevice, GS Baccarin, FMD Costa, RDS Fernandes, FA Aouada and MRD Moura. Combining chitosan nanoparticles and garlic essential oil as additive fillers to produce pectin-based nanocomposite edible films. *Polymers* 2023; **15(10)**, 2244.

[22] BA Joda, ZMA Al-Kadhim, HJ Ahmed and AKH Al-Khalaf. A convenient green method to synthesize β-carotene from edible carrot and nanoparticle formation. *Karbala International Journal of Modern Science* 2022; **8(1)**, 20-27.

[23] DSB Anugrah, LV Darmalim, JD Sinanu, R Pramitasari, D Subali, EA Prasetyanto and XT Cao. Development of alginate-based film incorporated with anthocyanins of red cabbage and zinc oxide nanoparticles as freshness indicator for prawns. *International Journal of Biological Macromolecules* 2023; **251(2)**, 126203.

[24] DK Alavijeh, B Heli and A Ajji. Development of a sensitive colorimetric indicator for detecting beef spoilage in smart packaging. *Sensors* 2024; **24(12)**, 3939.

[25] G Giyatmi, TAE Poetri, HE Irianto, D Fransiska and A Agusman. Effect of alginate and polyethylene glycol addition on physical and mechanical characteristics of K-carrageenan-based edible film. *Squalen Bulletin of Marine and Fisheries Postharvest and Biotechnology* 2020; **15(1)**, 41-51.

[26] S Sriwidodo, T Subroto, I Maksum, A Subarnas, B Kesumawardhany, DM Diah, D Lestari and AK

Umar. Preparation and optimization of chitosan-hEGF nanoparticle using ionic. *International Journal of Research in Pharmaceutical Sciences* 2020; **11(1)**, 1220-1230.

[27] BA Alimi, S Pathania, J Wilson, B Duffy and JMC Frias. Extraction, quantification, characterization, and application in food packaging of chitin and chitosan from mushrooms: A review. *International Journal of Biological Macromolecules* 2023; **237(3)**, 124195.

[28] L Suriati, IGP Mangku, GASW Krisnawati and AANS Girindra. The impact of chitosan at the physical performance of the coffee skin-based edible film. *Journal of Agriculture and Crops* 2023; **9(92)**, 156-163.

[29] SB Sasongko and FL Agustina. Stengthening of edible film from corn starch and iota carrageenan with butterfly pea flower extraction (*Clitoria ternate* L.) addition. *E3S Web of Conferences* 2024; **503(2)**, 09005.

[30] F Dai, Q Zhuang, G Huang, H Deng and X Zhang. Infrared spectrum characteristics and quantification of OH groups in coal. *ACS Omega* 2023; **8(19)**, 17064-17076.

[31] SB Rekik, S Gassara, J Bouaziz, S Baklouti and A Deratani. Performance enhancement of kaolin/chitosan composite-based membranes by cross-linking with sodium tripolyphosphate: Preparation and characterization. *Membranes* 2023; **13(2)**, 229.

[32] F Hong, P Qiu, Y Wang, P Ren, J Liu, J Zhao and D Gou. Chitosan-based hydrogels: From preparation to applications, a review. *Food Chemistry: X* 2024; **21(2)**, 101095.

[33] I Aranaz, AR Alcántara, MC Civera, C Arias, B Elorza, AH Caballero and N Acosta. Chitosan: An overview of its properties and applications. *Polymers* 2021; **13(19)**, 3256.

[34] CY Hsu, Y Ajaj, ZH Mahmoud, GK Ghadir, ZK Alani, MM Hussein, SA Hussein, MM Karim, A Al-khalidi, JK Abbas, AH Kareem and E Kianfar. Adsorption of heavy metal ions use chitosan/graphene nanocomposites: A review study. *Results in Chemistry* 2024; **7**, 101332.

[35] E Alehosseini, HS Tabarestani, MS Kharazmi and SM Jafari. Physicochemical, thermal, and morphological properties of chitosan nanoparticles produced by ionic gelation. *Foods* 2022; **11(23)**, 3841.

[36] ABD Nandiyanto, R Oktiani and R Ragadhita. How to read and interpret ftir spectroscope of organic material. *Indonesian Journal of Science and Technology* 2019; **4(1)**, 97-118.

[37] F Kokkinaki and SA Ordoudi. Insights into the FTIR spectral fingerprint of saffron (Crocus sativus L.) stigmas after gentle drying treatments. *Food Bioprocess Technology* 2023; **16(12)**, 3057-3072.

[38] R Román-Doval, SP Torres-Arellanes, AY Tenorio-Barajas, A Gómez-Sánchez and AA Valencia-Lazcano. Chitosan: Properties and its application in agriculture in context of molecular weight. *Polymers* 2023; **15(13)**, 2867.

[39] D Debnath, I Samal, C Mohapatra, S Routray, MS Kesawat and R Labanya. Chitosan: An autocidal molecule of plant pathogenic fungus. *Life* 2022; **12(11)**, 1908.

[40] JA Sirviö, AM Kantola, S Komulainen and S Filonenko. Aqueous modification of chitosan with itaconic acid to produce strong oxygen barrier film. *Biomacromolecules* 2021; **22(5)**, 2119-2128.

[41] G Riccucci, S Ferraris, C Reggio, A Bosso, G Örlygsson, CH Ng and S Spriano. Polyphenols from grape pomace: Functionalization of chitosan-coated hydroxyapatite for modulated swelling and release of polyphenols. *Langmuir* 2021; **37(51)**, 14793-14804.

[42] V Suryanti, T Kusumaningsih, D Safriyani and IS Cahyani. Synthesis and characterization of cellulose ethers from screw pine (Pandanus tectorius) leaves cellulose as food additives. *International Journal of Technology* 2023; **14(3)**, 659-668.

[43] MT Caccamo and S Magazù. Multiscale spectral analysis on lysozyme aqueous solutions in the presence of polyethyleneglycol. *Molecules* 2022; **27(24)**, 8760.

[44] Khairuddin, E Pramono, SB Utomo, V Wulandari, AW Zahrotul and F Clegg. FTIR studies on the effect of concentration of polyethylene glycol on polimerization of Shellac. *Journal of Physics: Conference Series* 2016; **776(1)**, 012053.

[45] M Ul-Islam, KF Alabbosh, S Manan, S Khan, F Ahmad and MW Ullah. Chitosan-based

nanostructured biomaterials: Synthesis, properties, and biomedical applications. *Advanced Industrial and Engineering Polymer Research* 2024; **7(1)**, 79-99.

[46] N Joudeh and D Linke. Nanoparticle classification, physicochemical properties, characterization, and applications: a comprehensive review for biologists. *Journal of Nanobiotechnology* 2022; **20(1)**, 262.

[47] KA Altammar. A review on nanoparticles: Characteristics, synthesis, applications, and challenges. *Frontiers in Microbiology* 2023; **14**, 1155622.

[48] AH Isaac, SYR Phillips, E Ruben, M Estes, V Rajavel, T Baig, C Paleti, K Landsgaard, RH Lee, T Guda, MF Criscitiello, C Gregory and DL Alge. Impact of PEG sensitization on the efficacy of PEG hydrogel-mediated tissue engineering. *Nature Communications* 2024; **15(1)**, 3283.

[49] MT Ekvall, I Gimskog, E Kelpsiene, A Mellring, A Månsson, M Lundqvist and T Cedervall. Nanoplastics released from daily used silicone and latex products during mechanical breakdown. *PLoS One* 2023; **18(9)**, e0289377.

[50] S Lee, LT Hao, J Park, DX Oh and DS Hwang. Nanochitin and nanochitosan: Chitin nanostructure engineering with multiscale properties for biomedical and environmental applications. *Advanced Materials* 2023; **35(4)**, 2203325.

[51] J Latupeirissa, M Tanasale, EG Fransina and A Noya. Synthesis and characterization of chitosan-citrate microparticle using ionic gelation methods. *Indonesian Journal of Chemical Research* 2022; **10(1)**, 1-7.

[52] NEA El-Naggar, AM Shiha, H Mahrous and ABA Mohammed. Green synthesis of chitosan nanoparticles, optimization, characterization and antibacterial efficacy against multi drug resistant biofilm-forming Acinetobacter baumannii. *Scientific Reports* 2022; **12(1)**, 19869.

[53] LH Zoe, SR David and R Rajabalaya. Chitosan nanoparticle toxicity: A comprehensive literature review of *in vivo* and *in vitro* assessments for medical applications. *Toxicology Reports* 2023; **11(1)**, 83-106.

[54] N Desai, D Rana, S Salave, R Gupta, P Patel, B Karunakaran, A Sharma, J Giri, D Benival and N Kommineni. Chitosan: A potential biopolymer in drug delivery and biomedical applications. *Pharmaceutics* 2023; **15(4)**, 1313.

[55] I Sánchez-Ortega, BE García-Almendárez, EM Santos-López, A Amaro-Reyes, JE Barboza-Corona and C Regalado. Antimicrobial edible films and coatings for meat and meat products preservation. *Scientific World Journal* 2014; **2014**, 248935.

[56] M Moura-Alves, A Esteves, M Ciríaco, JA Silva and C Saraiva. Antimicrobial and antioxidant edible films and coatings in the shelf-life improvement of chicken meat. *Foods* 2023; **12(12)**, 2308.